

# Bidirectional Coupling of two Duffing-type Circuits

Ch. K. VOLOS, I. M. KYPRIANIDIS, and I. N. STOUBOULOS

Physics Department  
 Aristotle University of Thessaloniki  
 Thessaloniki, 54124  
 GREECE

*Abstract:* - In this paper we have studied experimentally the case of chaotic synchronization of two identical nonlinear electric circuits. This is a very interesting research area because of its applications to the field of secure communications. The circuit we have used is a second order, Duffing-type, nonlinear electric circuit driven by a sinusoidal voltage source. The nonlinear element has a cubic i-v characteristic of the form,  $i(v) = p \cdot v + q \cdot v^3$ . We have studied the dynamic behavior of the system in the case of the bidirectional coupling via a linear resistor. Both experimental and simulation results have shown that chaotic synchronization is possible.

*Key-Words:* - Chaos, Duffing equation, Chaotic synchronization, Bidirectional coupling.

## 1 Introduction

Synchronization, among dynamical variables in coupled chaotic systems would appear to be almost an oxymoron as the definition of chaos. Since the beginning of the '90s, many researchers have discussed the synchronization of two coupled chaotic systems [1-4]. Synchronization of chaotic systems plays an important role in several research areas. For example, neural signals in the brain are observed to be chaotic and it is worth to consider further their possible synchronization [5]. Other interesting examples may be seen from the working artificial neural networks [6], biological networks [7], coupled chaotic neurons [8], multimode lasers [9], coupled map lattices [10, 11], and coupled electric oscillators [12]. Also, the topic of synchronization has risen great interest as a potential mean in communication [13, 14]. The last few years, a considerable effort has been devoted to extend the chaotic communication applications to the field of secure communications.

Generally, there are two methods of chaos synchronization available in the literature. In the first method, a stable subsystem of a chaotic system could be synchronized with a separate chaotic system, under certain suitable conditions. The second method to achieve chaos synchronization between two identical nonlinear systems is due to the effect of resistive coupling without requiring to construct any stable subsystem [15-17]. As we know from the bibliography, periodically forced synchronized chaotic circuits are much more noise-resistant than autonomous synchronized chaotic circuits.

In this paper we have studied the case of bidirectional coupling of two identical, second order Duffing-type electrical oscillators.

## 2 The Duffing-Type Circuit

Duffing's equation,

$$\frac{d^2x_1}{dt^2} + \varepsilon \cdot \frac{dx_1}{dt} + a \cdot x_1 + b \cdot x_1^3 = B \cdot \cos(\omega \cdot t) \quad (1)$$

is one of the most famous and well studied nonlinear non-autonomous equations, exhibiting various dynamic behaviors, including chaos and bifurcations. One of the simplest implementations of the Duffing equation has been presented by Kyprianidis et al. [18]. It is a second order nonlinear circuit, which is excited by a sinusoidal voltage source and contains two op-amps (LF411) operating in the linear region Fig.1. This circuit has also a very simple nonlinear element, implementing a cubic function of the form

$$i(v) = p \cdot v + q \cdot v^3 \quad (2)$$

which is shown in Fig.2.

Denoting by  $x_1$  and  $x_2$  the voltages across capacitors  $C_2$  and  $C_4$  respectively, we have the following state equations.

$$\frac{dx_1}{dt} = -\frac{1}{C_2 \cdot R_2} \cdot x_1 + \frac{1}{C_2 \cdot R_3} \cdot x_2 \quad (3)$$

$$\frac{dx_2}{dt} = -\frac{R_0}{C_4 \cdot R_5} \cdot f(x_1) + \frac{V_0}{C_4 \cdot R_5} \cdot \cos(\omega \cdot t) \quad (4)$$

where,  $f(x_1) = p \cdot x_1 + q \cdot x_1^3$ , is a cubic function.

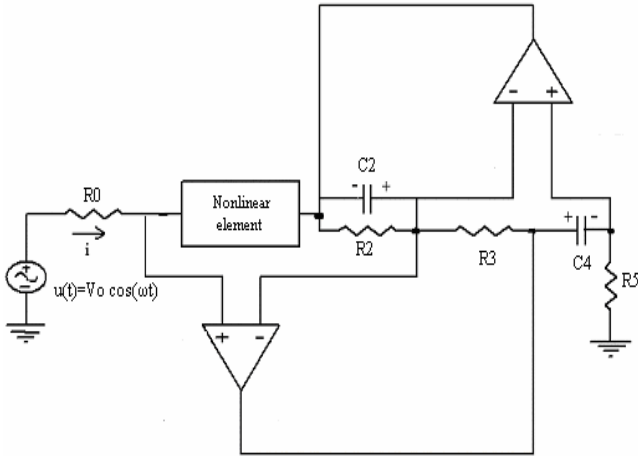


Fig.1. The electric circuit obeying Duffing's equation.

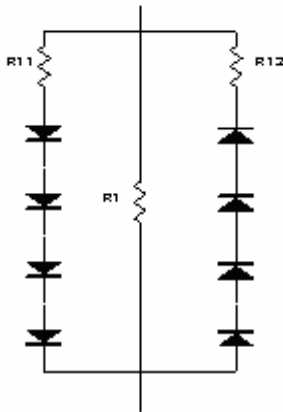


Fig.2. The nonlinear element implementing the cubic function of the form  $i(v) = p \cdot v + q \cdot v^3$

Finally, from equations (3) and (4), we take the Duffing equation (1), where,

$$\begin{aligned} \epsilon &= \frac{1}{C_2 \cdot R_2}, & a &= \frac{p \cdot R_0}{C_2 \cdot C_4 \cdot R_3 \cdot R_5} \\ b &= \frac{r \cdot R_0}{C_2 \cdot C_4 \cdot R_3 \cdot R_5}, & B &= \frac{V_0}{C_2 \cdot C_4 \cdot R_3 \cdot R_5} \end{aligned} \quad (5)$$

The values of circuit parameters are  $R_0=2.05k\Omega$ ,  $R_2=5.248k\Omega$ ,  $R_3=R_5=1k\Omega$ ,  $R_{11}=R_{12}=0.557k\Omega$ ,  $R_1=8.11k\Omega$ ,  $C_2=105.9nF$ ,  $C_4=9.79nF$ ,  $V_0=2V$  and  $f=1.273kHz$ , so the normalized parameters take the following values  $a=0.25$ ,  $b=1$ ,  $\epsilon=0.18$ ,  $\omega=0.8$  and  $B=20$ . The phase portrait of  $x_2$  vs.  $x_1$  is shown in Fig.3, where we can see that the circuit has a chaotic behavior.

### 3 The Coupled System

The system of two identical Duffing circuits bidirectionally or two-way coupled via a linear resistor  $R_c$  is shown in Fig.4.

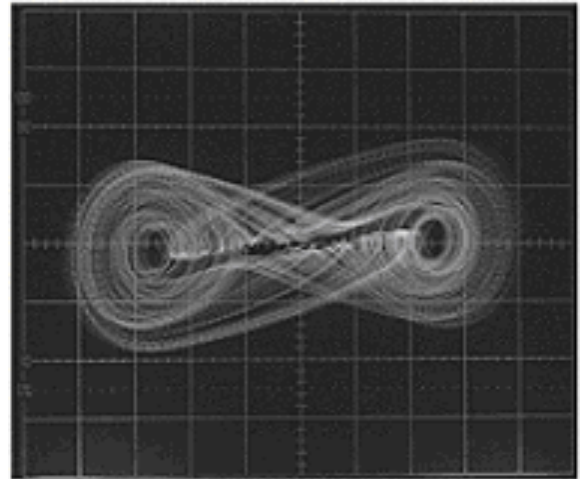


Fig.3. Experimental phase portrait of  $x_2$  vs.  $x_1$  for  $a=0.25$ ,  $b=1$ ,  $\epsilon=0.18$ ,  $\omega=0.8$  and  $B=20$  (Horiz.: 1V/div., Vert.: 5V/div.)

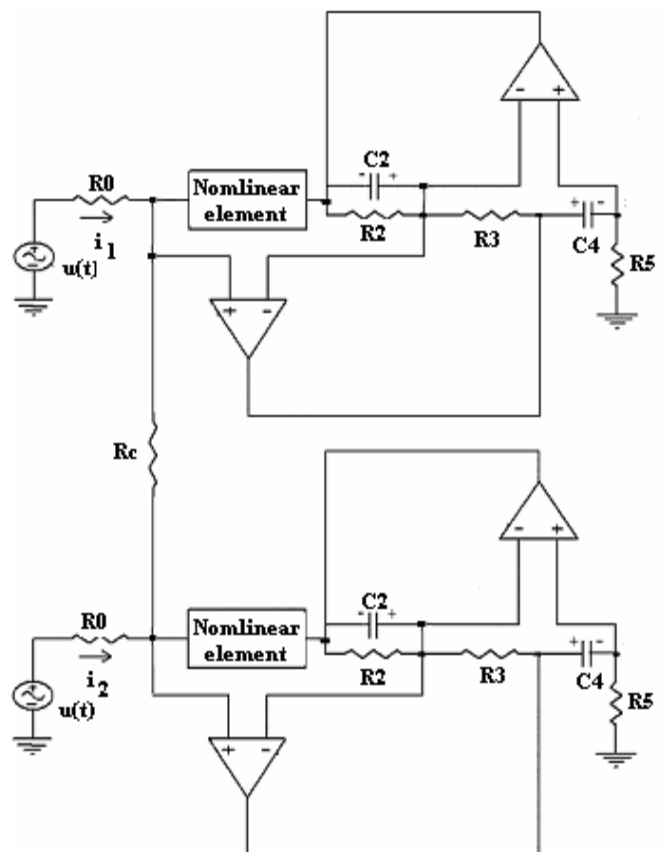


Fig.4. Two Duffing circuits bidirectionally coupled via a linear resistor.

The state equations of the system of Fig.4 has the form of equations (6-9), or the form of equations (10, 11), where,  $x_1 = v_{C_2}$ ,  $x_2 = v_{C_4}$ ,  $\dot{x}_1 = \dot{v}_{C_2}$ ,  $\dot{x}_2 = \dot{v}_{C_4}$ , and  $\xi = \frac{R_0}{R_c + 2R_0}$ , is the coupling factor.

We have chosen the following values of the normalized parameters,  $a=0.25$ ,  $b=1$ ,  $\epsilon=0.18$ ,  $\omega=0.8$

and  $B=20$ , so the single circuit is in a chaotic steady state, as we saw before.

$$\frac{dx_1}{dt} = -\frac{1}{C_2 R_2} x_1 + \frac{1}{C_2 R_3} x_2 \quad (6)$$

$$\frac{dx_2}{dt} = -\frac{R_0}{C_4 R_5} f(x_1) + \frac{q}{C_4 R_5} \cos(\omega t) - \frac{R_0^2}{C_4 R_5 (R_c + 2R_0)} (f(x'_1) - f(x_1)) \quad (7)$$

$$\frac{dx'_1}{dt} = -\frac{1}{C_2 R_2} x'_1 + \frac{1}{C_2 R_3} x'_2 \quad (8)$$

$$\frac{dx'_2}{dt} = -\frac{R_0}{C_4 R_5} f(x'_1) + \frac{q}{C_4 R_5} \cos(\omega t) - \frac{R_0^2}{C_4 R_5 (R_c + 2 \cdot R_0)} (f(x_1) - f(x'_1)) \quad (9)$$

$$\frac{d^2 x_1}{dt^2} + \varepsilon \frac{dx_1}{dt} + \alpha(1 - \xi)x_1 + b(1 - \xi)x_1^3 + \alpha \xi x'_1 + b \xi (x'_1)^3 = B \cdot \cos(\omega t) \quad (10)$$

$$\frac{d^2 x'_1}{dt^2} + \varepsilon \frac{dx'_1}{dt} + \alpha(1 - \xi)x'_1 + b(1 - \xi)(x'_1)^3 + \alpha \xi x_1 + b \xi x_1^3 = B \cdot \cos(\omega t) \quad (11)$$

The two single circuits have different initial conditions and we study the dynamics of the system, as the coupling coefficient  $\xi$  is increased from zero (uncoupled circuits).

### 4 Chaotic Synchronization

Considering the case, that the two coupled circuits are identical and are driven by signals of the same amplitude, we have studied chaotic synchronization as the coupling factor  $\xi$  is increased. The bifurcation diagram  $x_1 - x'_1$  versus  $\xi$  is shown in Fig.5. When the difference  $x_1 - x'_1$  becomes equal to zero, this means that the two circuits are in chaotic synchronization.

In Figs.6-14 we can see the experimental results from the coupled system for various values of the coupling resistor  $R_c$ . The system has a variety of dynamical behavior as we saw at the bifurcation diagram (Fig.5). We observe that the system appears phase-locked states of period-1, period-2, e.t.c. in different ranges of values of the coupling factor  $\xi$  (Figs.6, 8, 9, 12). Also, the system passes from chaotic states (Figs.7, 10, 11, 13) to a chaotic synchronization (Fig.16) as we expect from the bifurcation diagram. The phenomenon of chaotic synchronization appears for  $\xi > 0.48$ . So, the coupled circuits confirmed the theoretical results we took from the simulation of the dynamical system, as

we saw in Figs.6, 11, 12, 14.

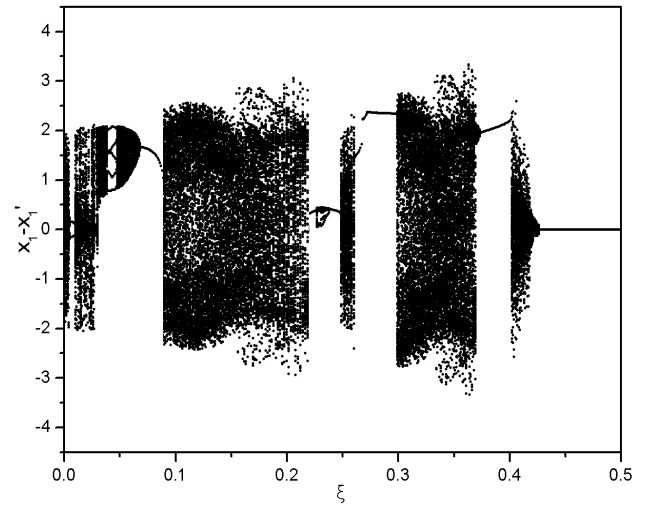
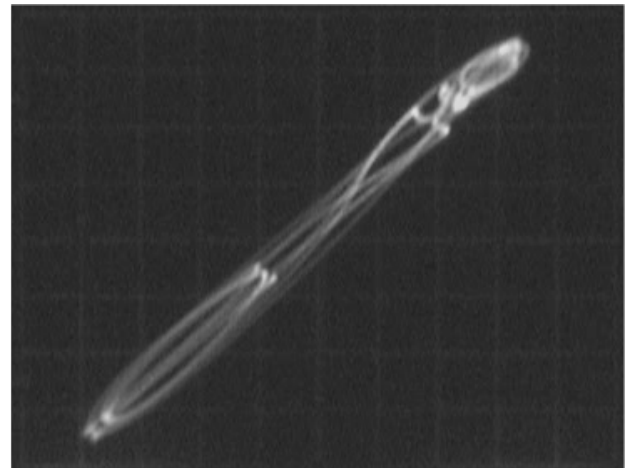
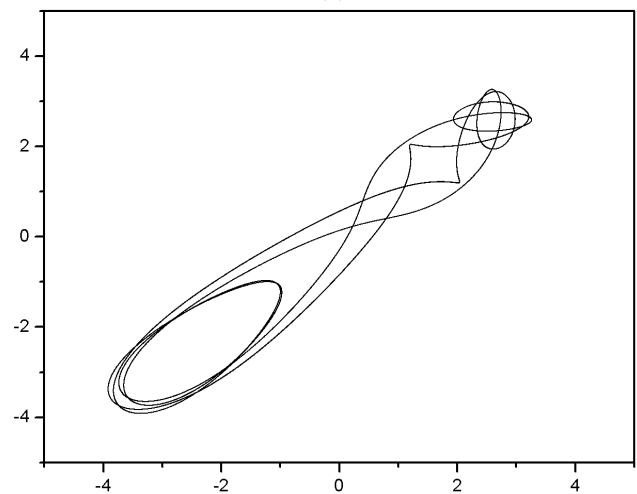


Fig.5. The bifurcation diagram  $x_1 - x'_1$  versus  $\xi$  for  $a=0.25, b=1, \varepsilon=0.18, \omega=0.8$  and  $B=20$ .



(a)



(b)

Fig.6. (a) Experimental phase portrait  $x'_1$  versus  $x_1$  (Horiz.  $V_{C2}$ : 1V/div., Vert.  $V_{C2}$ : 1V/div.), (b) Theoretical phase portrait  $x'_1$  versus  $x_1$ , for  $R_c=182k\Omega$  ( $\xi=0.011$ ). The system is in period-2.

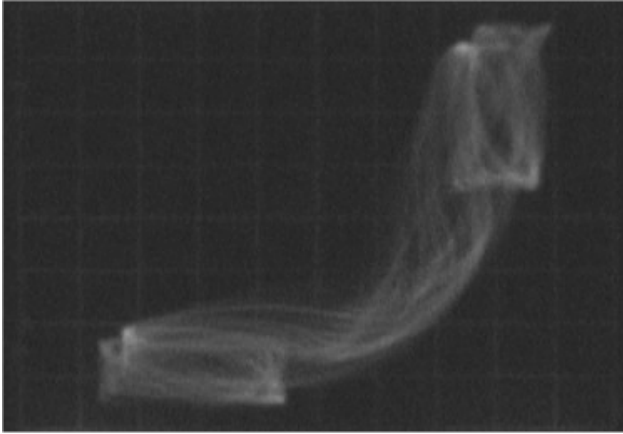


Fig.7. Experimental phase portrait  $x_1'$  versus  $x_1$  for  $R_C=54k\Omega$  ( $\xi=0.035$ ).  
(Horiz.  $V_{C2}$ : 1V/div., Vert.  $V_{C2}'$ : 1V/div.).  
The system is in a chaotic state.

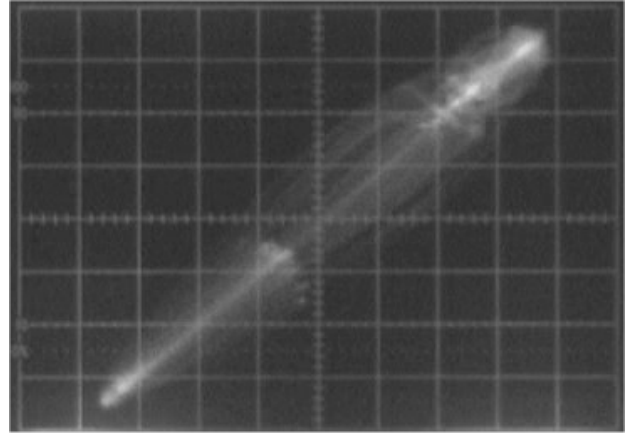


Fig.10. Experimental phase portrait  $x_1'$  versus  $x_1$  for  $R_C=5k\Omega$  ( $\xi=0.23$ ).  
(Horiz.  $V_{C2}$ : 1V/div., Vert.  $V_{C2}'$ : 1V/div.).  
The system is in a chaotic state.

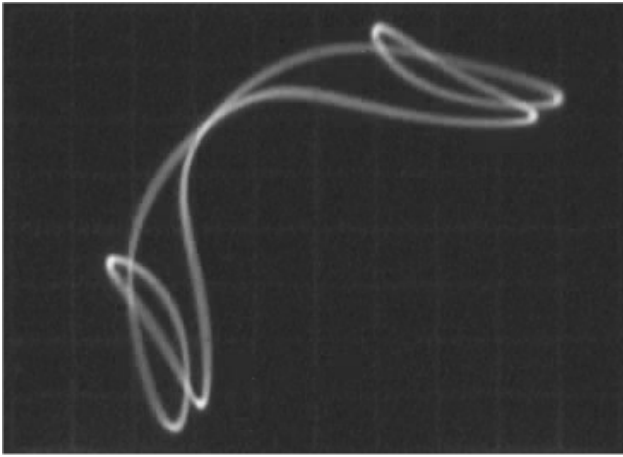
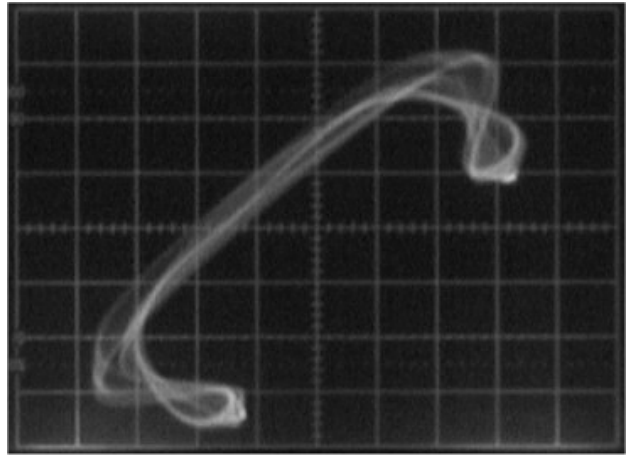


Fig.8. Experimental phase portrait  $x_1'$  versus  $x_1$  for  $R_C=41k\Omega$  ( $\xi=0.08$ ).  
(Horiz.  $V_{C2}$ : 1V/div., Vert.  $V_{C2}'$ : 1V/div.).  
The system is in period-1 state.



(a)

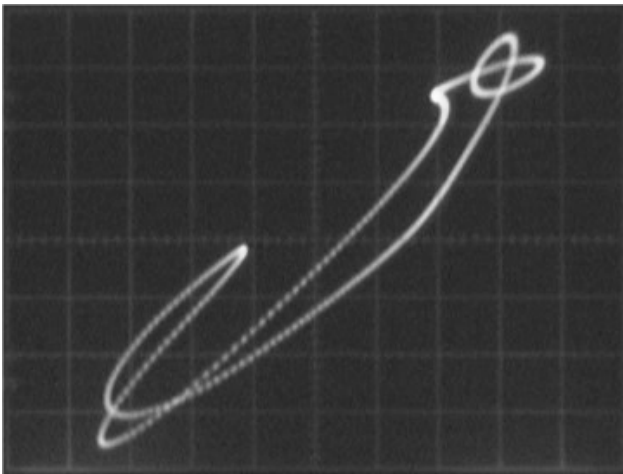
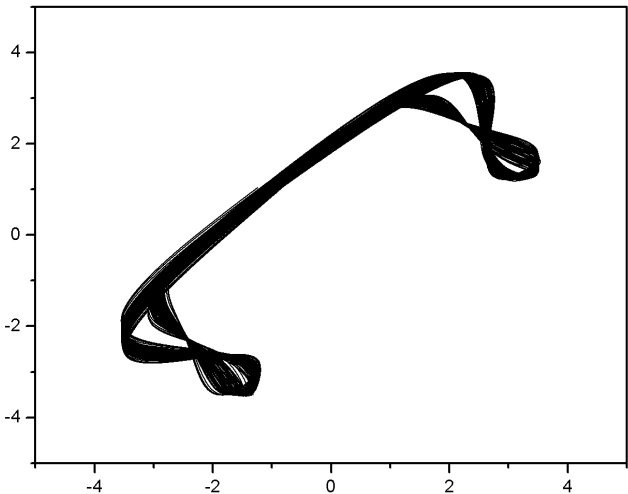
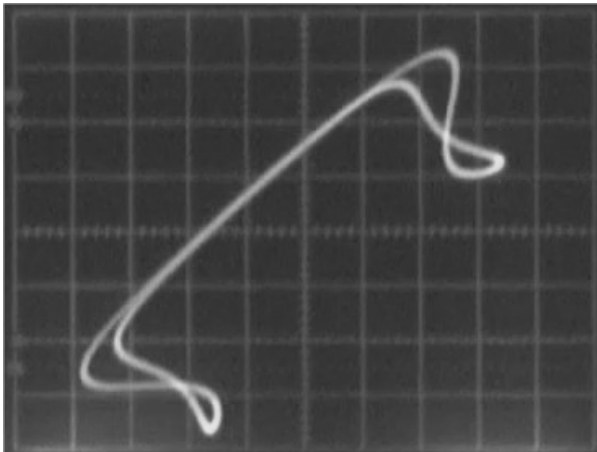


Fig.9. (a) Experimental phase portrait  $x_1'$  versus  $x_1$  for  $R_C=5.2k\Omega$  ( $\xi=0.22$ ). (Horiz.  $V_{C2}$ : 1V/div., Vert.  $V_{C2}'$ : 1V/div.). The system is in a period-1 state.

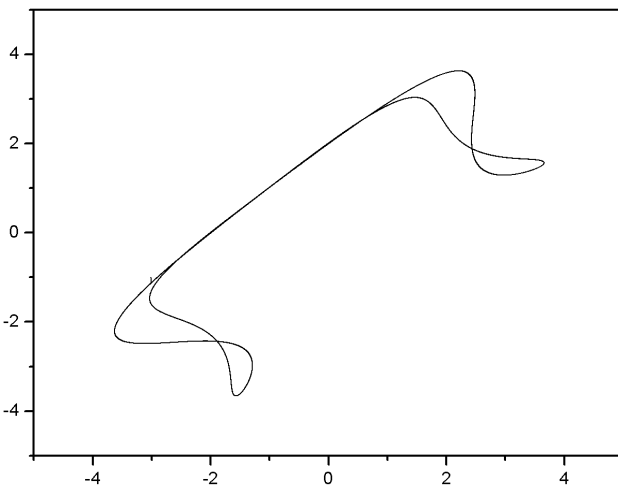


(b)

Fig.11. (a) Experimental phase portrait  $x_1'$  versus  $x_1$  (Horiz.  $V_{C2}$ : 1V/div., Vert.  $V_{C2}'$ : 1V/div.),  
(b) Theoretical phase portrait  $x_1'$  versus  $x_1$ , for  $R_C=1.3k\Omega$  ( $\xi=0.38$ ) The system is in a chaotic state.

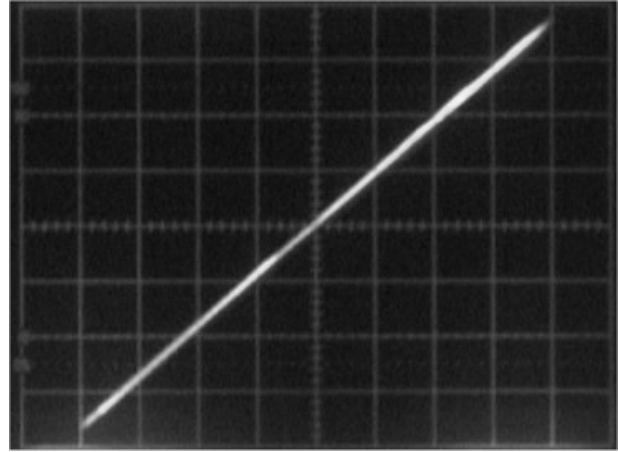


(a)

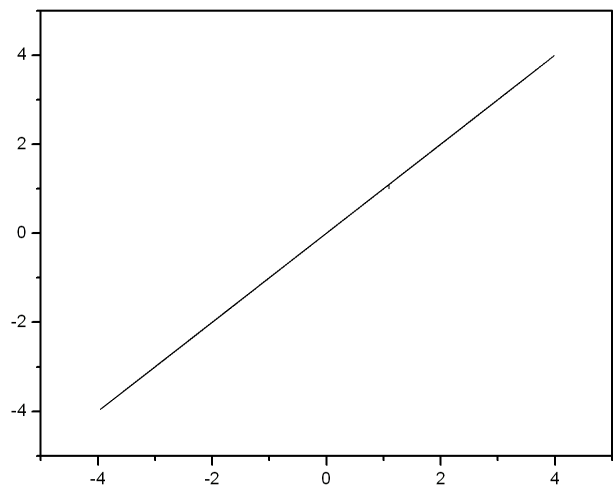


(b)

Fig.12. (a) Experimental phase portrait  $x_1'$  versus  $x_1$  (Horiz.  $V_{C2}$ : 1V/div., Vert.  $V_{C2}'$ : 1V/div.), (b) Theoretical phase portrait  $x_1'$  versus  $x_1$ , for  $R_C=1k\Omega$  ( $\xi=0.4$ ). The system is in period-1 state.



(a)



(b)

Fig.14. (a) Experimental phase portrait  $x_1'$  versus  $x_1$  (Horiz.  $V_{C2}$ : 1V/div., Vert.  $V_{C2}'$ : 1V/div.), (b) Theoretical phase portrait  $x_1'$  versus  $x_1$ , for  $R_C=170\Omega$  ( $\xi=0.48$ ). The system is in a chaotic synchronization.

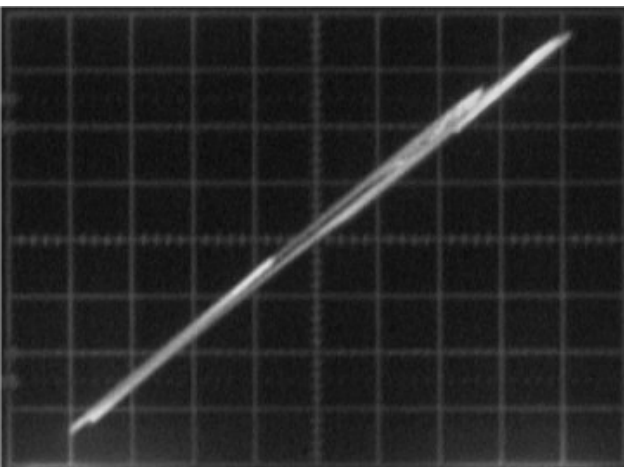


Fig.13. Experimental phase portrait  $x_1'$  versus  $x_1$  for  $R_C=260\Omega$  ( $\xi=0.47$ ). (Horiz.  $V_{C2}$ : 1V/div., Vert.  $V_{C2}'$ : 1V/div.). The system is in a chaotic state.

## 5 Conclusion

In this paper we have studied the dynamics of two resistively coupled nonlinear Duffing-type electrical oscillators. The two circuits are identical, having chaotic dynamical behavior, as we have found out from both theoretical and experimental results. We experimentally confirmed the expected behavior of the system for various values of the coupling resistor  $R_C$ . We have shown periodic and chaotic states, in different ranges of values of the coupling factor  $\xi$ . Finally, we observed a chaotic synchronization when the coupling factor  $\xi > 0.48$ .

### References:

- [1] Brown R., Kocarev L., A Unifying Definition of Synchronization for Dynamical Systems, *Chaos*,

- Vol. 10, 2000, pp. 344–349.
- [2] Boccaletti S., Kurths J., Osipov G., Valladares D.L., Zhou C.S., The Synchronization of Chaotic Systems, *Phys. Rep.* Vol. 366, 2002, pp.1–101.
- [3] Jiang G., Tang W., Chen G., A Simple Global Synchronization Criterion for Coupled Chaotic Systems" *Chaos, Solitons & Fractals*, Vol. 15(5), 2003, pp.925–935.
- [4] Wu, C. W., *Synchronization in Coupled Chaotic Circuits and Systems*, World Scientific, 2002.
- [5] Tass, P., Roseblum, M.G., Weule, M.G., Kurths, J., Pikovsky, A., Volkman, J., Schnitzler, A., Freund, H.J., Detection of n:m Phase Locking from Noise Data: Application to Magnetoencephalography, *Phys. Rev. Lett.*, Vol. 81, 1998, pp. 3291-3294.
- [6] Schäfer, C., Roseblum, M.G., Kurths, J., Abel, H.H., Heartbeat Synchronized with Ventilation, *Nature*, Vol. 392, 1998, pp.239-240.
- [7] Neiman, A., Xing Pei, Russell, D., Wojtenek, W., Wilkens, L., Moss, F., Braun, H. A., Huber, M. T., and Voigt, K., Synchronization of the Noisy Electrosensitive Cells in the Paddlefish, *Phys. Rev. Lett.*, Vol. 82, 1999, pp. 660–663.
- [8] Bazhenov, M., Huerta, R., Rabinovich, M. I. and Sejnowski, T., Cooperative Behavior of a Chain Synaptically Coupled Chaotic Neurons, *Physica D*, Vol. 116, 1998, pp. 392-400.
- [9] Van Wiggeren, G. D. and Roy, R., Communication with Chaotic Lasers, *Science*, Vol. 279, 1998, pp. 1198-1200.
- [10] Meng Zhan, Gang Hu, and Junzhong Yang, Synchronization of Chaos in Coupled Systems, *Phys. Rev. E*, Vol. 62, 2000, pp. 2963-2966.
- [11] Wang Jinlan, Chen Guangzhi, Qin Tuanfa, Ni Wansun, and Wang Xuming, Synchronizing spatiotemporal chaos in coupled map lattices via active-passive decomposition, *Phys. Rev. E*, Vol. 58, 1998, pp. 3017-3021.
- [12] Kyprianidis, I. M and Stouboulos, I. N., Chaotic Synchronization of Two Resistively Coupled Nonautonomous and Hyperchaotic Oscillators, *Chaos Solitons and Fractals*, Vol. 17, 2003, pp. 317-325.
- [13] Callegari, S., Rovatti, R. and Setti, G. Spectral properties of chaos-based FM signals: Theory and simulation results, *IEEE Trans. Circuits Syst. I*, Vol. 50, 2003, pp. 3–15.
- [14] Tse, C.K. and Lau, F., *Chaos-based Digital Communication Systems: Operating Principles, Analysis Methods, and Performance Evaluation*, Berlin, New York: Springer Verlag, 2003.
- [15] Kyprianidis I. M., Volos Ch. K. and Stouboulos I. N., Suppression of Chaos by Linear Resistive Coupling, *WSEAS Trans. Circ. Syst.*, Vol 4, 2005, pp. 527-534.
- [16] Kyprianidis, I. M. and Stouboulos I. N., Dynamics of two Resistively Coupled Duffing-type electrical Oscillators, *International Journal of Bifurcation and Chaos*, Vol.16, No.6, 2006, pp. 1765-1775.
- [17] Kyprianidis, I. M. and Stouboulos I. N., Chaotic Synchronization of three Coupled Oscillators with Ring Connection, *Chaos Solit. Fract.*, Vol.47, 2003, pp. 1349-1351.
- [18] Kyprianidis, I. M., Volos, Ch. K. and Stouboulos, I. N. Experimental Study of a Nonlinear Circuit Described by Duffing's Equation, Science and Engineering, *Journal of Istanbul Kultur University*, Volume 4, No. 4, December 2006, pp. 45-54.